Performance Analysis of Mixed FSO/RF System for Satellite-Terrestrial Relay Network

Qiang Sun *Member, IEEE*, Qi Hu, Yiyang Wu, Xiaomin Chen, Jiayi Zhang *Senior Member, IEEE* and Miguel López-Benítez *Senior Member, IEEE*

***Abstract*—This paper analyzes the performance of a satellite-terrestrial free-space optical (FSO)/millimeter wave (MMW) radio frequency (RF) relaying system with amplify-and-forward (AF) and decode-and-forward (DF) relaying. The Málaga ($\mathcal{M}$) distribution with pointing error impairments and the multi-cluster fluctuating two-ray (MFTR) fading model are introduced to characterize the FSO link for both heterodyne detection (HD) and indirect modulation/direct detection (IM/DD) and MMW link, respectively. Therefore, the precise closed-form expression of end-to-end signal-to-noise ratio (SNR) for the outage probability (OP), average bit error rate (BER), ergodic capacity (EC) and effective capacity (EFC) is derived. In addition, we present an asymptotical result analysis for the OP and average BER at high SNR in terms of simple functions. Finally, we employ Monte-Carlo (MC) simulation results to verify all our analytical results.**

***Index Terms*—Amplify-and-forward, decode-and-forward, satellite-terrestrial relay system, Málaga ($\mathcal{M}$) distribution, multi-cluster fluctuating two-ray fading.**

I. Introduction

With the high-quality demands of communication services, terrestrial cellular networks struggle to achieve the requirements of communication [1]. Satellite networks will provide global services, especially for users in remote areas [2], [3]. A geostationary Earth orbit (GEO) satellite, which can offer the widest range of coverage and does not require frequent handovers, is a popular type deployed in satellite communication systems. Compared to terrestrial communication systems, satellite-terrestrial relay systems have the advantages of high cost-effectiveness and wide coverage [4]. Due to the features of satellite-terrestrial systems, they have been recognized as promising systems in future wireless communication [5]. In particular, these hybrid networks are especially well-suited for emergency and disaster relief communications, navigation systems, and providing connectivity to remote areas where traditional communication infrastructure is unavailable [6]. Although line-of-sight (LOS) satellites and terrestrial systems are commonly used in the above conditions, mountains, buildings, reefs and shadows can block the LOS [7]. Furthermore, multi-path effect caused by scattering may produce many non-LOS signals in the vicinity of receiver. The effect even can cause the communication link to drop under extreme weather like floods, hurricanes, and earthquakes [8]. To solve the above issues, free-space optical (FSO)/radio frequency (RF) relaying systems are considered as an effective technique. The FSO systems are suitable for the satellite-terrestrial communication with several advantages of huge optical bandwidth, narrow beam divergence, unlicensed spectrum and high security [9]. Nevertheless, optical signal propagation is severely influenced by the dynamic air environment, which induces atmospheric turbulence and pointing errors [10]. To assure the high reliability of the communication, RF systems are considered in the vicinity of terrestrial receivers. For RF systems, the millimeter wave (MMW) RF link follows multi-cluster fluctuating two-ray (MFTR) fading, which is the generalization and harmonization of both fluctuating two-ray (FTR) and $\kappa-\mu$ fading models, which are assumed to investigate the multi-path effect caused by scattering. This generalization means that the FTR fading model obtains the additional multi-path clusters, and has two fluctuating specular components in $\kappa-\mu$ fading [11]. Furthermore, the MFTR fading model has both the bimodality [12] and asymptotic decay [13] properties from FTR and $\kappa-\mu$ fading, respectively. The physical formulations of the two fading models are variable, which means they cannot have the same behaviors of propagation. The MFTR fading can reconcile the two dominant approaches and the statistics formulations are as tractable as other models. To ensure the stable transmission between satellite and terrestrial, the mixed FSO/MMW model with Málaga ($\mathcal{M}$) model and MFTR fading are proposed in our work, which can effectively deal with the afore-mentioned issues [14]. The mixed satellite-terrestrial FSO/RF relaying systems performance can be improved significantly with the best features of FSO and RF communication technologies.

A. Related Works

As shown in Table I, varying fading models have been employed in various studies to analyze the performance of relay systems [14]— [31]. Most existing works studied under the assumption of decode-and-forward (DF) [19], [21], [22], [24], [25], [27], [29], [31] and amplify-and-forward (AF) relays which encompass fixed-gain [14], [15], [19], [26], [27], [28], [30] and channel state information (CSI)-assisted [14], [17], [23], [26]. In the FSO link, fading caused by

Q. Sun, Q. Hu, Y. Wu and X. Chen are with the School of Information Science and Technology, Nantong University, Nantong 226019, China.(e-mail: sunqiang@ntu.edu.cn).

J. Zhang is with the School of Electronic and Information Engineering, Beijing Jiaotong University, Beijing 100044, China. (e-mail: jiayizhang@bjtu.edu.cn).

Miguel López-Benítez is with the Department of Electrical Engineering and Electronics,University of Liverpool, Liverpool L69 3GJ, U.K., and alsowith the ARIES Research Centre, Antonio de Nebrija University, 28040 Madrid, Spain (e-mail: m.lopez-benitez@liverpool.ac.uk).

TABLE I: Literature of FSO/RF Systems

Ref.	System Model	Relay Model	FSO Link	RF Link	Performance Metrics
[14]	hybrid FSO/RF relay system for satellite-terrestrial relay network	fixed-gain AF; CSI-Assisted AF	Shadowed Rician	Nakagami-m	average SER
[15]	mixed RF/FSO relay system	fixed-gain AF	Generalized Málaga ($\mathcal{M}$)	Rayleigh	average SER
[16]	mixed RF/FSO relay system	variable gain relay	Fisher-Snedecor F	$\kappa-\mu$	BER,EC
[17]	mixed FSO/RF relay system	CSI-Assisted AF	Exponentiated Weibull	$\alpha-\mu$	ASC, SOP, PNSC
[18]	mixed RF/FSO relay system	fixed gain relay; variable gain relay	Exponentiated Weibull	Nakagami-m	OP, SER, EC
[19]	mixed RF/THz relay system	fixed-gain AF;DF	$\alpha-\mu$	$\eta-\mu_1$	OP, average BER, ACC
[20]	mixed FSO/RF relay system	AF	Málaga ($\mathcal{M}$)	Shadowed $\kappa-\mu$	OP, average SEP
[21]	hybrid FSO/RF relay system	DF	Málaga ($\mathcal{M}$)	Beaulieu-Xie	OP, average BER, EC
[22]	mixed FSO/RF relay system	DF	DGG	Nakagami-m	OP, BER, EC
[23]	mixed RF/FSO relay system	CSI-Assisted AF	DGG	Nakagami-m	OP, BER, EC
[24]	hybrid FSO/RF system	DF	GG	Nakagami-m	OP, average BER
[25]	mixed FSO/RF relay system	DF	GG	Rayleigh	OP, EC, asymptotic BER
[26]	hybrid FSO/RF system	fixed-gain AF; CSI-Assisted AF	GG	Rayleigh	OP, BER
[27]	mixed RF/FSO relay system	fixed-gain AF;DF	GG	α-$\mathcal{F}$	OP, average BER, EC, EFC
[28]	hybrid satellite-terrestrial relay network	fixed-gain AF	Shadow Rician	Nakagami-m	EC, average SER
[29]	hybrid FSO/RF space–air–ground integrated network	DF	Generalized Málaga ($\mathcal{M}$)	κ-μ	OP, average SER, EC, OC
[30]	mixed satellite-terrestrial relay network	fixed-gain AF	GG	Shadow Rician	COP, SOP
[31]	Hybrid RF-FSO Satellite-Aerial-Terrestrial Networks	DF	GG	Nakagami-m	SOP

atmospheric turbulence and pointing errors is experienced. The Gamma-Gamma (GG) distribution [24]—[27], [30], [31] is considered as the most typical distribution for the irradiance, and the Málaga ($\mathcal{M}$) distribution [20]—[21] is presented in [32] to model the variability in irradiance of an infinite optical wavefront as it propagates through turbulent media across all levels of irradiance. Some authors also investigated the performance of shadowed Rician fading [14], [28], Generalized Málaga ($\mathcal{M}$) [15], [29], Fisher-Snedecor F [16], Exponentiated Weibull [17], [18], $\alpha-\mu$ [19] and Double generalized gamma [22], [23]. Most works employed the heterodyne detection (HD) and indirect modulation/direct detection (IM/DD), which are significant techniques for FSO link. The IM/DD is simpler than HD, but the sensitivity of heterodyne detection performs better. On the RF side, Nakagami-m [14], [18], [22]—[24], [28], [31], and Rayleigh [15], [25], [26], are commonly assumed, as well as $\kappa-\mu$ [16], $\alpha-\mu$ [17], $\eta-\mu$ [19], shadowed $\kappa-\mu$ [20], [29], Beaulieu-Xie [21] and α-$\mathcal{F}$ [27]. Although [14] analyzed relaying systems in the case of satellite-terrestrial links, the study falls short in accurately analyzing the multi-path effect caused by scattering and the random fluctuations suffered by the receiver side of the system. Note that most works only investigated the performance metrics of outage probability (OP) [18]—[27], [29], bit error rate (BER) [16], [19], [21]—[23], and ergodic capacity (EC) [16], [18], [21]—[23], [25], [27]—[29]. The significant metric of effective capacity (EFC) is seldom considered to verify the system performance. In our work, we analyze the EFC and deal with the aforemationed issues by investigating mixed FSO/RF systems with RF link which undergoes the MFTR distribution. The MFTR fading model recently proposed in [11] is more flexible at propagation features than other conventional channel models. Furthermore, the MFTR fading encompasses several typically fading models such as Nakagami-m, Rayleigh, Rician and FTR as either special or limiting cases. Moreover, Málaga ($\mathcal{M}$) distribution can be reduced to many popular fading models, such as GG and lognormal distributions [33]. Different from the GG distribution, Málaga ($\mathcal{M}$) distribution can present a wider reflection for all turbulence conditions. Therefore, this work presents a more general and comprehensive study that not only considers a broader range of performance metrics but also a more general range of channel fading conditions compared to previous work.

We emphasize the key contributions of our work as follows:

1) We consider a mixed satellite-terrestrial FSO/MMW relaying system model for wireless communications with Málaga ($\mathcal{M}$) and MFTR fading distributions under link budget and path loss.
2) Using both HD and IM/DD detection techniques, the closed-form expressions of the cumulative distribution function (CDF) of SNR and other system metrics namely OP, average BER, EC and EFC are derived.
3) Based on fixed-gain AF and DF relays, the effects of system performance are analyzed under different parameters (i.e., atmospheric turbulence, detection techniques, pointing error impairments, fading figures, amount of clusters and optical power).
4) Closed-form asymptotic expressions of the performance metrics are provided at high SNR regime. Finally, the diversity gain is derived to clarify the crucial effects of the relaying system under various channel parameters and schemes.

B. Organization

The remainder of this work is presented as follows. First, we detail the channel and the satellite-terrestrial system in Section II. The closed-form formulations and asymptotic analysis of the CDF of SNR are clarified in Section III. We provide the exact expressions for OP, average BER, EC, EFC and their asymptotic results at high SNRs in Section IV. Section V presents Monte-Carlo (MC) simulation and numerical results. Finally, Section VI is the conclusion of this work. In addition, the proofs for several statistical properties are provided in three appendices.

Notation: In our work, we use $f_{(.)}(.)$, $F_{(.)}(.)$ to describe the probability density function (PDF) and CDF, respectively; $\mathbb{E}[.]$ denotes expectation; $\approx$ refers to "approximately equal to"; In addition, $\Gamma(.)$ is the gamma function [34, Eq. (8.310)]; ${}_2F_1(\cdot)$ is the Gauss hypergeometric function [34, Eq. (9.111)]; $G_{p,q}^{m,n}[\cdot]$ is the Meijer's G-function [35, Eq. (1.112)]; $H(\cdot)$ represents the Fox's-H function [35, Eq. (1.2), Eq. (1.3)].

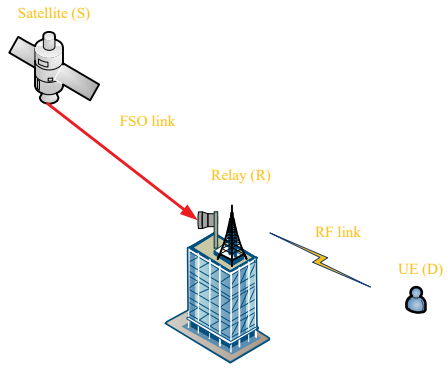

Fig. 1: The satellite-terrestrial FSO/MMW system model.

II. System and Channel Models

In this paper, a mixed satellite-terrestrial FSO/MMW model is considered as shown in Fig. 1. Note that the LOS link becomes unavailable due to the obstructing buildings causing a heavy shadow and an unfavorable link environment. The dynamic movement effect for signal transmission caused by a GEO satellite is assumed to be negligible in this work [28]. Therefore, the satellite and user are considered as source transmitter (S) as well as destination receiver (D), which are connected by relay R with AF and DF relays. The S and D both have a single antenna [28]. Similar assumptions have been often made in previous related work. Presume the FSO link experiences a Málaga ($\mathcal{M}$) distribution with pointing errors of both HD and IM/DD, whereas the RF link follows MFTR fading, which includes the special cases for $\kappa-\mu$ ($\Delta=0$) and FTR ($\mu=1$) models [11].

A. FSO link

The channel from the satellite to the relay can be represented as

$$h_{\mathrm{FSO}} = P_{\mathrm{FSO}}\eta_{\mathrm{FSO}}I \tag{1}$$

where P_{FSO} and η_{FSO} denote the average transmitted optical power and the propagation loss, encompassing the impacts of path loss, satellite beam pattern, and receiver noise in the FSO link, respectively. The propagation loss, η_{FSO}, is characterized as follows

$$\eta_{FSO} = \frac{C\sqrt{G_S G_R}}{4\pi f_{FSO} d_{SR}\sqrt{\kappa T B_{FSO}}} \tag{2}$$

where C represents the speed of light, G_R denotes the receive gain, and the satellite beam gain $G_S = G_{\max}\left(\frac{J_1(u)}{2u}+36\frac{J_3(u)}{u^3}\right)^2$ [36], where $G_{\max}$ denotes the maximum beam gain, and $u = 2.07123\frac{\sin\varphi}{\sin\varphi_{3dB}}$. Here, φ is the angle between the location of the corresponding receiver and the beam center with respect to the satellite, and φ_{3dB} is the 3-dB angle. Additionally, f_{FSO} represents the carrier frequency, d_{SR} is the distance between S and R. The receiver noise can be expressed as $\kappa T B_{FSO}$, where $\kappa = 1.38\times10^{-23}J/K$ is the Boltzmann constant, T is the receiver noise temperature, and B_{FSO} is the carrier bandwidth [37].

The PDF of the receiver irradiance I is provided by [38, Eq. (10)]

$$f_I(I) = \frac{\zeta^2 A_1}{2I}\sum_{t=1}^{\beta} b_t \mathrm{G}_{1,3}^{3,0}\left[\frac{\alpha\beta}{(g\beta+\Omega')}\frac{I}{I_l A_0}\;\middle|\;\begin{matrix}\zeta^2+1\\ \zeta^2,\alpha,t\end{matrix}\right], \tag{3}$$

where

$$\begin{aligned} A_1 &\triangleq \frac{2\alpha^{\frac{\alpha}{2}}}{g^{1+\frac{\alpha}{2}}\Gamma(\alpha)}\left(\frac{g\beta}{g\beta+\Omega'}\right)^{\frac{\beta+\alpha}{2}}\\ b_t &= a_t\left[\frac{\alpha\beta}{g\beta+\Omega'}\right]^{-\frac{\alpha+t}{2}}\\ a_t &\triangleq \binom{\beta-1}{t-1}\frac{(g\beta+\Omega')^{1-\frac{t}{2}}}{(t-1)!}\left(\frac{\Omega'}{g}\right)^{t-1}\left(\frac{\alpha}{\beta}\right)^{\frac{t}{2}}\\ \Omega' &= \Omega+2b_0\rho+2\sqrt{2b_0\rho\Omega}\cos(\phi_A-\phi_B) \end{aligned}, \tag{4}$$

where ζ means the ratio of the equivalent beam radius at the receiver. There are three components accepted at the receiver constituent to the channel coefficient of Málaga ($\mathcal{M}$) distributions which can described as $I = I_a I_p$, where I_a denotes the impact of atmospheric turbulence-induced fading, respectively. I_p is the geometric spread and pointing errors. α is the amount of large-scale cells, β is the number of large-scale cells of fading parameter [38]. The average power of the total scatter components is $2b_0$, while the average power of the scattering component, which is represented by $g = 2b_0(1-\rho)$, where the $\rho\in[0,1]$ stands for the amount of scattering power coupled to the LOS term. Moreover, Ω represents the average power of the LOS term, the variables ϕ_A and ϕ_B indicate the deterministic phases of LOS term and the scatter terms coupled-to-LOS. The average SNR of both types of detections is given by

$$\begin{aligned} \mu_{\mathrm{HD}} &= \frac{\eta_e\mathbb{E}_I[I]}{N_0} = \frac{I_l A_0\eta_e\zeta^2(g+\Omega')}{(1+\zeta^2)N_0}\\ \mu_{\mathrm{IM/DD}} &= \frac{\eta_e^2\mathbb{E}_I^2[I]}{N_0} = \frac{I_l^2 A_0^2\eta_e^2\zeta^4(g+\Omega')^2}{(1+\zeta^2)^2 N_0} \end{aligned}, \tag{5}$$

where η_e is the effective photoelectric conversion ratio. We assume $I_l = 1$ in this paper. With instantaneous SNR $\gamma_{HD} = \frac{\eta_e I}{N_0}$ and $\gamma_{\mathrm{IM/DD}} = \frac{\eta_e^2 I^2}{N_0}$, we obtain $I = \frac{I_l A_0\zeta^2(g+\Omega')\gamma_{HD}}{\mu_{\mathrm{HD}}(\zeta^2+1)}$ and $I = \frac{\zeta^2(g+\Omega')I_l A_0}{(\zeta^2+1)\sqrt{\frac{\gamma_{\mathrm{IM/DD}}}{\mu_{\mathrm{IM/DD}}}}}$, respectively. The N_0 is additive white Gaussian noise. Substituting (5) into (3), the PDF of Málaga ($\mathcal{M}$) distribution for S-R link is drawn as

$$f_{\gamma_{FSO}}^{S-R}(\gamma) = \frac{\zeta^2 A_1}{2^r\gamma}\sum_{t=1}^{\beta} b_t \mathrm{G}_{1,3}^{3,0}\left[B\left(\frac{\gamma}{\mu_r}\right)^{\frac{1}{r}}\;\middle|\;\begin{matrix}\zeta^2+1\\ \zeta^2,\alpha,t\end{matrix}\right], \tag{6}$$

where

$$B = \frac{\zeta^2\alpha\beta(g+\Omega')}{(\zeta^2+1)(g\beta+\Omega')}, \tag{7}$$

μ_r is the average electrical SNR. The parameter r represents the detection methods of HD and IM/DD:

$$\begin{aligned} r=1,\mu_1 &= \overline{\gamma}_{HD} = \mu_{HD}\\ r=2,\mu_2 &= \frac{\zeta^2(\zeta^2+1)^{-2}(\zeta^2+2)(g+\Omega')}{\alpha^{-1}(\alpha+1)\left[2g(g+2\Omega')+\Omega'^2(1+\frac{1}{\beta})\right]}\overline{\gamma}_{\mathrm{IM/DD}} \end{aligned}, \tag{8}$$

Substituting (6) into $F_{\gamma_{\mathrm{FSO}}}(\gamma) \triangleq \int_0^{\gamma} f_{\gamma_{\mathrm{FSO}}}(x)dx$ and using [35, Eq.(1.59)] with some algebraic transformations, we can

derive the CDF of instantaneous SNR γ_{FSO} of Málaga ($\mathcal{M}$) distribution for S-R link as

$$F_{\gamma_{FSO}}^{S-R}(\gamma) = 1 - \frac{\zeta^2 A_1 r}{2^r} \sum_{t=1}^{\beta} b_t \times H_{2,4}^{4,0}\left[\begin{matrix} \left(\zeta^2+1, r\right) (1,1) \\ (0,1), \left(\zeta^2, r\right), (\alpha, r), (t, r) \end{matrix} \middle| \frac{B^r \gamma}{\mu_r} \right]. \quad (9)$$

B. RF link

The channel from the relay to the user can be illustrated as

$$h_{\text{RF}} = P_{\text{RF}} \eta_{\text{RF}} g_{\text{RF}} \quad (10)$$

where P_{RF} and η_{RF} denote the transmitted RF power and the average power gain of the RF link, encompassing the impacts of antenna gain, oxygen attenuation, and the receiver noise of the RF link. The propagation loss, η_{FSO}, is modeled as follows [39]

$$\eta_{RF} = \frac{G_{RF}}{\sigma_{RF}^2} = \frac{G_t + G_r - 20\log_{10}\left(\frac{4\pi d_{RD}}{\lambda_{RF}}\right) - a_{oxy} d_{RD} - a_{rain} d_{RD}}{\sigma_{RF}^2} \quad (11)$$

where G_t and G_r denote the transmit antenna gain and receive antenna gain, respectively. The noise variance $\sigma_{RF}^2 = B_{RF} N_{1_{RF}} + N_{RF}$ [40], with bandwidth B_{RF}, noise power spectral density $N_{1_{RF}}$, and the noise figure of the RF receiver N_{RF}. The a_{oxy} and a_{rain} represent the attenuation coefficients due to oxygen absorption and rain scattering, respectively. The fading gain g_{RF} can be modeled using the MFTR distribution.

Assuming that the SNR of R-D link, γ_{RF}, undergoes the MFTR fading, the PDF is provided by [11, Eq. (16)]

$$f_{\gamma_{RF}}^{R-D}(x) = \sum_{i=0}^{\infty} w_i f_X^{\text{G}}\left(\mu + i; \frac{\bar{\gamma}(\mu+i)}{\mu(K+1)}; x\right), \quad (12)$$

where

$$f_X^{\text{G}}(\lambda; \nu; y) = \frac{\lambda^\lambda}{\Gamma(\lambda)\nu^\lambda} y^{\lambda-1} \exp\left(-\frac{\lambda y}{\nu}\right), \quad (13)$$

and

$$w_i = \frac{\Gamma(m+i)(\mu K)^i m^m}{\Gamma(m)\Gamma(i+1)} \frac{(1-\Delta)^i}{\sqrt{\pi}(\mu K(1-\Delta)+m)^{m+i}} \times \sum_{q=0}^{i} \binom{i}{q} \frac{\Gamma\left(q+\frac{1}{2}\right)}{\Gamma(q+1)} \left(\frac{2\Delta}{1-\Delta}\right)^q \times {}_2F_1\left(m+i, q+\frac{1}{2}; q+1; \frac{-2\mu K\Delta}{\mu K(1-\Delta)+m}\right), \quad (14)$$

where K is the average power ratio of dominant specular component to the remaining diffused multi-path. $m \in R^+$ is the channel parameter and $\Delta \in [0,1]$ represents the similarity of received powers from the specular components. Note that when $\Delta = 0$, the MFTR model corresponds to the $\kappa - \mu$ shadowed model. Furthermore, μ denotes the number of clusters, where the MFTR model reduces to FTR fading model for $\mu = 1$ [11]. Using [41, Eq. (2.9.4), Eq. (2.9.1)], the PDF of MFTR fading for R-D link can be expressed as

$$f_{\gamma_{RF}}^{R-D}(\gamma) = \sum_{i=0}^{\infty} \frac{w_i}{\Gamma(\mu+i)\gamma} G_{0,1}^{1,0}\left[\frac{\mu(K+1)\gamma}{\bar{\gamma}} \middle| \begin{matrix} - \\ \mu+i \end{matrix}\right], \quad (15)$$

Applying (15) into the identity $F_{\gamma_{\text{RF}}}(\gamma) \triangleq \int_0^\gamma f_{\gamma_{\text{RF}}}(x)dx$, we obtain the R-D link CDF of γ_{RF}

$$F_{\gamma_{RF}}^{R-D}(\gamma) = 1 - \sum_{i=0}^{\infty} \frac{w_i}{\Gamma(\mu+i)} \times \int_\gamma^\infty \gamma^{-1} H_{0,1}^{1,0}\left[\frac{\mu(K+1)\gamma}{\bar{\gamma}} \middle| \begin{matrix} - \\ (\mu+i, 1) \end{matrix}\right] d\gamma, \quad (16)$$

Using [35, Eq. (2.54)] and with some mathematical manipulations, the CDF of MFTR distribution (16) becomes

$$F_{\gamma_{RF}}^{R-D}(\gamma) = 1 - \sum_{i=0}^{\infty} \frac{w_i}{\Gamma(\mu+i)} \times H_{1,2}^{2,0}\left[\begin{matrix} (1,1) \\ (0,1)\,(\mu+i, 1) \end{matrix} \middle| \frac{\mu(K+1)\gamma}{\bar{\gamma}} \right]. \quad (17)$$

III. End-To-End SNR Statistics Characteristics

We derive the closed-form formulations with AF and DF relay of the mixed FSO/MMW model exactly. The asymptotic CDF at high SNR are also presented in this section.

A. End-to-End SNR

During each transmission period, two signaling intervals are delineated: In the initial signaling interval, the received signal at R undergoes multiplication by a gain factor G [42]. Subsequently, in the second signaling interval, it is retransmitted to D. Assuming that S transmits a signal with an average power normalized to unity, the instantaneous end-to-end SNR at the destination, denoted as γ^{AF}, is expressed as $\gamma^{AF} = \frac{\left(\alpha_{FSO}^2/N_{0_{FSO}}\right)\left(\alpha_{RF}^2/N_{0_{RF}}\right)}{\left(\alpha_{RF}^2/N_{0_{RF}}\right)+\left(1/G^2 N_{0_{FSO}}\right)}$ [43], where α_{FSO} and α_{RF} represent the fading amplitudes of the wireless channels in the $S-R$ and $R-D$ links, respectively. $N_{0_{FSO}}$ and $N_{0_{RF}}$ denote the power of the AWGN component at the input of the relay and the destination, and G stands for the relay gain. If $Q = \frac{1}{G^2 N_{0_{FSO}}}$, $\gamma i = \frac{\alpha i^2}{N_{0_i}}$ for $i = FSO, RF$. Consequently, the end-to-end SNR of AF relay can be simplified to [30, Eq. (1)]

$$\gamma^{AF} = \frac{\gamma_{\text{FSO}}\gamma_{\text{RF}}}{\gamma_{\text{RF}} + Q}, \quad (18)$$

where Q represents a constant numerical value which has relation to the fixed gain AF. When the DF relaying is employed, the S-D link SNR is provided by [44, Eq. (7)]

$$\gamma^{DF} = \min(\gamma_{\text{FSO}}, \gamma_{\text{RF}}). \quad (19)$$

B. CDF of SNR for AF Relaying

1) Closed-form Expression: Based on the SNR in (18) of S-D link, the CDF of AF relaying for a mixed satellite-terrestrial FSO/mmWave system can be formulated as closed-form (20) with the help of the bivariate Fox's-H function.

Proof: Please see Appendix A. ■

In (20), $H_{p1,q1:p2,q2:p3,q3}^{0,n1:m2,n2:m3,n3}[\cdot]$ denotes the extended generalized bivariate Fox's H function, which can be calculated numerically with the help of well-known software like MATHEMATICA [45]. The function can be implemented in MATLAB as well. Specially, for the R-D link, the MFTR fading corresponds to FTR for $\mu = 1$. When $\Delta = 0, K \to \infty$ and $\mu = 1$, the MFTR fading simplifies to the Nakagami-m

$$F_{\gamma^{AF}}^{S-D}(\gamma)=1-\frac{\zeta^2 A_1}{2^r}\sum_{t=1}^{\beta}b_t\sum_{i=0}^{\infty}\frac{w_i}{\Gamma(\mu+i)}H_{1,0;2,0;3,2}^{0,1;0,2;0,3}\left[\begin{array}{c}(1;-1,\frac{1}{r})\\ -\\ (1;1),(1-\mu-i;1)\\ -\\ (1-\zeta^2,1),(1-\alpha,1),(1-t,1)\\ (0,\frac{1}{r}),(-\zeta^2,1)\end{array}\middle|\begin{array}{c}\\ \\ \frac{\bar{\gamma}}{\mu(K+1)Q},\frac{1}{B}\left(\frac{\mu_r}{\gamma}\right)^{\frac{1}{r}}\\ \\ \\ \end{array}\right], \quad (20)$$

fading model. For S-R link, when $\rho=1,\Omega'=1$, the Málaga ($\mathcal{M}$) fading model can be reduced to the GG distribution. Furthermore, setting $\rho=1,\Omega'=1$ and $\mu=1$, we have the closed-form expression of dual-hop GG/FTR system in [46, Eq. (10)].

Since the SNR of the satellite-terrestrial relaying systems is improved in various technologie, it is important to deduce the asymptotic results with AF relaying of the CDF at high average SNRs. After performing some algebraic manipulations to (20) with [45, Eq. (1.1)] and utilizing [41, Eq. (1.5.9), Eq. (1.8.4)], the following asymptotic formulation can be obtained

$$F_{\gamma^{AF}}^{\infty}(\gamma)\approx\frac{\zeta^2 A_1}{2^r}\sum_{t=1}^{\beta}b_t\sum_{i=0}^{\infty}\frac{w_i}{\Gamma(\mu+i)}\sum_{j=1}^{4}\Psi_j{\mu_r}^{-\theta_j}, \quad (21)$$

where $\theta_{j=1}^{4}=\left\{\frac{\zeta^2}{r},\frac{\alpha}{r},\frac{t}{r},\frac{\mu+i}{r}\right\}$

$$\Psi_1=\Gamma\left(\alpha-\zeta^2\right)\Gamma\left(t-\zeta^2\right)(B^r\gamma)^{\frac{\zeta^2}{r}}\times\left(\frac{\Gamma\left(\mu+i-\frac{\zeta^2}{r}\right)}{\zeta^2}\left(\frac{\mu(K+1)Q}{\bar{\gamma}}\right)^{\frac{\zeta^2}{r}}+\frac{\Gamma(\mu+i)}{\zeta^2}\right), \quad (22)$$

$$\Psi_2=\frac{1}{(\zeta^2-\alpha)}\Gamma(t-\alpha)(B^r\gamma)^{\frac{\alpha}{r}}\times\left(\frac{\Gamma\left(\mu+i-\frac{\alpha}{r}\right)}{\alpha}\left(\frac{\mu(K+1)Q}{\bar{\gamma}}\right)^{\frac{\alpha}{r}}+\frac{\Gamma(\mu+i)}{\alpha}\right), \quad (23)$$

$$\Psi_3=\frac{1}{(\zeta^2-t)}\Gamma(\alpha-t)(B^r\gamma)^{\frac{t}{r}}\times\left(\frac{\Gamma\left(\mu+i-\frac{t}{r}\right)}{t}\left(\frac{\mu(K+1)Q}{\bar{\gamma}}\right)^{\frac{t}{r}}+\frac{\Gamma(\mu+i)}{t}\right), \quad (24)$$

$$\Psi_4=\frac{1}{(\zeta^2-(\mu+i)r)(\mu+i)}\Gamma(\alpha-(\mu+i)r)\times\Gamma(t-(\mu+i)r)\left(\frac{\mu(K+1)Q}{\bar{\gamma}}\right)^{\mu+i}(B^r\gamma)^{\frac{\mu+i}{r}}. \quad (25)$$

Proof: Please see Appendix B. ■

2) Truncation error: We provide the truncation error as shown on the top of the next page by limiting (20) to the first N_1 terms. The truncation error of $F_\gamma(\gamma)$ relative to the first N_1 terms is as

$$\varepsilon(N_1)=F_\gamma(\infty)-\hat{F}_\gamma(\infty). \quad (27)$$

To validate the convergence of the series mentioned in (20), Table II provides the corresponding values of N_1 for different channel parameters. As it can be observed, we can obtain a satisfactory accuracy with less than 120 terms.

TABLE II: Necessary conditions N_1 for the truncation error ($\varepsilon_1<10^{-3}$) under varying numerical K, m and Δ.

System and channel parameters	N_1	ε_1
$K=15,m=5,\Delta=0.1$	110	2.7×10^{-4}
$K=10,m=2,\Delta=0.5$	108	2.1×10^{-4}
$K=10,m=0.3,\Delta=0.5$	111	6.2×10^{-4}

C. CDF of SNR for DF Relaying

Due to the SNR of the variable-gain relaying system, which is represented by $\gamma=\frac{\gamma_{RF}\gamma_{FSO}}{\gamma_{RF}+\gamma_{FSO}+1}\cong\min(\gamma_{RF},\gamma_{FSO})$ [26], we consider DF relaying in our paper.

1) Closed-form Expression: The CDF of $\gamma_{\text{DF}}=\min(\gamma_{\text{FSO}},\gamma_{\text{RF}})$ at the receiver can be described with individual CDFs of both S-R and R-D link as [27, Eq. (12)] by using (19)

$$\begin{aligned}F_{\gamma^{DF}}^{S-D}(\gamma)&=F_{\gamma_{\text{FSO}}}^{S-R}(\gamma)+F_{\gamma_{\text{RF}}}^{R-D}(\gamma)-F_{\gamma_{\text{FSO}}}^{S-R}(\gamma)F_{\gamma_{\text{RF}}}^{R-D}(\gamma)\\&=1-F_{\gamma_{\text{FSO}}}^{C}(\gamma)F_{\gamma_{\text{RF}}}^{C}(\gamma)\end{aligned}, \quad (28)$$

where $F_\gamma^C(\cdot)$ represents the complementary CDF (CCDF) of the instantaneous SNR [46]. We can rewrite the CDF of γ_{DF} for S-D link as

$$F_{\gamma^{DF}}^{S-D}(\gamma)=1-\frac{\zeta^2 A_1 r}{2^r}\sum_{t=1}^{\beta}b_t\sum_{i=0}^{\infty}\frac{w_i}{\Gamma(\mu+i)}\times H_{2,4}^{4,0}\left[\frac{B^r\gamma}{\mu_r}\middle|\begin{array}{c}(\zeta^2+1,r),(1,1)\\(0,1),(\zeta^2,r),(\alpha,r),(t,r)\end{array}\right]\times H_{1,2}^{2,0}\left[\frac{\mu(K+1)\gamma}{\bar{\gamma}}\middle|\begin{array}{c}(1,1)\\(0,1)(\mu+i,1)\end{array}\right], \quad (29)$$

Proof: By inserting (9) and (17) into (28) and after some algebraic transformation, we have the CDF as shown in (29). Thus, the proof is completed. ■

By applying [41, Eq. (1.5.9), Eq. (1.8.4)] to (29), the asymptotic CDF of mixed FSO/MMW model at high average SNRs for DF scheme can be expressed as

$$F_{\gamma^{DF}}^{\infty}(\gamma)=F_{\gamma_{\text{FSO}}}^{\infty}(\gamma)+F_{\gamma_{\text{RF}}}^{\infty}(\gamma)-F_{\gamma_{\text{FSO}}}^{\infty}(\gamma)F_{\gamma_{\text{RF}}}^{\infty}(\gamma), \quad (30)$$

where

$$\begin{aligned}F_{\gamma_{FSO}}^{\infty}(\gamma)&=\frac{\zeta^2 A_1 r}{2^r}\sum_{t=1}^{\beta}b_t\frac{(\alpha-\zeta^2)\Gamma(t-\zeta^2)}{\zeta^2}\Gamma\left(\frac{B^r\gamma}{\mu_r}\right)^{\frac{\zeta^2}{r}}\\&+\frac{\zeta^2 A_1 r}{2^r}\sum_{t=1}^{\beta}b_t\frac{1}{\alpha(\zeta^2-\alpha)}\Gamma(t-\alpha)\left(\frac{B^r\gamma}{\mu_r}\right)^{\frac{\alpha}{r}}\\&+\frac{\zeta^2 A_1 r}{2^r}\sum_{t=1}^{\beta}b_t\frac{1}{t(\zeta^2-t)}\Gamma(\alpha-t)\left(\frac{B^r\gamma}{\mu_r}\right)^{\frac{t}{r}}\end{aligned}, \quad (31)$$

$$F_{\gamma_{RF}}^{\infty}(\gamma)=\sum_{i=0}^{\infty}\frac{w_i}{\Gamma(\mu+i)(\mu+i)}\left(\frac{\mu(K+1)\gamma}{\bar{\gamma}}\right)^{\mu+i}. \quad (32)$$

$$\hat{F}_{\gamma^{AF}}^{S-D}(\gamma)=1-\frac{\zeta^2 A_1}{2^r}\sum_{t=1}^{\beta} b_t \sum_{i=0}^{N_1}\frac{w_i}{\Gamma(\mu+i)} H_{1,0;2,0;3,2}^{0,1;0,2;0,3}\left[\begin{array}{c|c} \begin{array}{c}(1;-1,\frac{1}{r})\\ -\\ (1;1),(1-\mu-i;1)\\ -\\ (1-\zeta^2,1),(1-\alpha,1),(1-t,1)\\ (0,\frac{1}{r}),(-\zeta^2,1)\end{array} & \frac{\bar{\gamma}}{\mu(K+1)Q},\frac{1}{B}\left(\frac{\mu_r}{\gamma}\right)^{\frac{1}{r}}\end{array}\right], \tag{26}$$

2) Truncation error: By limiting (32) to the first N_2 terms, we can obtain

$$\hat{F}_{\gamma_{RF}}^{\infty}(\gamma)=\sum_{i=0}^{N_2}\frac{w_i}{\Gamma(\mu+i)(\mu+i)}\left(\frac{\mu(K+1)\gamma}{\bar{\gamma}}\right)^{\mu+i}. \tag{33}$$

Similarly, the terms N_2 presented in (33) with various performance metrics confirm the convergence of series in Table III. The satisfactory accuracy can be achieved for all considered cases with less than 30 terms (e.g., for an error smaller than 10^{-4}).

TABLE III: Necessary conditions N_2 for the truncation error ($\varepsilon_1 < 10^{-4}$) with variable numerical K, m and Δ.

System and channel parameters	N_2	ε_1
$K=15, m=5, \Delta=0.1$	20	1.7×10^{-5}
$K=10, m=2, \Delta=0.5$	24	1.8×10^{-5}
$K=10, m=0.3, \Delta=0.5$	27	3.1×10^{-5}

IV. Performance Analysis

A. Outage Probability

Ensuring that the instantaneous SNR γ is below a predetermined protection ratio γ_{th} can obtain the OP. The OP of S-R link can be derived by substituting γ_{th} into (20), we have

$$\begin{aligned} P_{out}(\gamma_{\text{th}}) &= \Pr\left[\gamma_{AF}<\gamma_{th}\right] \\ &= \Pr\left[\frac{\gamma_{FSO}\gamma_{RF}}{\gamma_{RF}+Q}<\gamma_{th}\right], \\ &= F_{\gamma^{AF}}^{S-D}(\gamma) \end{aligned} \tag{34}$$

Similarly, the OP of R-D link can be formulated as

$$\begin{aligned} P_{out}(\gamma_{\text{th}}) &= \Pr\left[\gamma_{DF}<\gamma_{th}\right] \\ &= \Pr\left[\min\left(\gamma_{FSO},\gamma_{RF}\right)<\gamma_{th}\right]. \\ &= F_{\gamma^{DF}}^{S-D}(\gamma) \end{aligned} \tag{35}$$

B. Average Bit-Error Rate

Another crucial metric of system performance is the average BER. For a different binary modulation schemes employed in different relaying systems, the average BER can be written as

$$\bar{P}_e=\frac{\delta}{2\Gamma(p)}\sum_{k=1}^{n} q_k^p\int_0^{\infty}\gamma^{p-1}\exp\left(-q_k\gamma\right)F_{\gamma}(\gamma)\,d\gamma, \tag{36}$$

where the modulation schemes are determined by the numerical values of parameters δ, n, p, q_k. The average BER of (36) for $\delta=1, n=1, p=0.5, q_k=1$ corresponds to coherent binary phase shift keying (CBPSK). When $\delta=1, n=1, p=1, q_k=1$, the system employs differential binary phase shift keying (DBPSK) scheme.

1) AF Relaying: Inserting (20) into (36) and after some numerical transformation, the average BER of S-D link can be expressed as (37) on the top of next page.

Proof: Please see Appendix C. ■

When we set $\rho=1, \Omega'=1$ and $\mu=1$, the average BER of S-D link in (37) reduces to [46, Eq. (27)], where the S-R link experiences GG for HD and IM/DD with pointing error impairments as well as the R-D link follows FTR model. Utilizing [45, Eq. (1.1)], [41, Eq. (1.5.9), Eq. (1.8.4)] and after some mathematical manipulations to (37), the asymptotic result is written as

$$\bar{P}_e^{AF}\approx\frac{\zeta^2 A_1}{2^r}\sum_{t=1}^{\beta}\sum_{i=0}^{\infty}\frac{b_t w_i}{\Gamma(\mu+i)}\frac{\delta}{2\Gamma(p)}\sum_{j=1}^{4}\Phi_j\Gamma(p+\theta_j), \tag{38}$$

where

$$\begin{aligned}\Phi_1 &= \Gamma\left(\alpha-\zeta^2\right)\Gamma\left(t-\zeta^2\right)\left(\frac{q_k\mu_r}{B^r}\right)^{-\frac{\zeta^2}{r}} \\ &\times\left(\frac{1}{\zeta^2}\Gamma\left(\mu+i-\frac{\zeta^2}{r}\right)\left(\frac{\bar{\gamma}}{\mu(K+1)Q}\right)^{-\frac{\zeta^2}{r}}+\frac{\Gamma(\mu+i)}{\zeta^2}\right),\end{aligned} \tag{39}$$

$$\begin{aligned}\Phi_2 &= \frac{1}{(\zeta^2-\alpha)}\Gamma(t-\alpha)\left(\frac{q_k\mu_r}{B^r}\right)^{-\frac{\alpha}{r}} \\ &\times\left(\frac{1}{\alpha}\Gamma\left(\mu+i-\frac{\alpha}{r}\right)\left(\frac{\bar{\gamma}}{\mu(K+1)Q}\right)^{-\frac{\alpha}{r}}+\frac{\Gamma(\mu+i)}{\alpha}\right),\end{aligned} \tag{40}$$

$$\begin{aligned}\Phi_3 &= \frac{1}{(\zeta^2-t)}\Gamma(\alpha-t)\left(\frac{q_k\mu_r}{B^r}\right)^{-\frac{t}{r}} \\ &\times\left(\frac{1}{t}\Gamma\left(\mu+i-\frac{t}{r}\right)\left(\frac{\bar{\gamma}}{\mu(K+1)Q}\right)^{-\frac{t}{r}}+\frac{\Gamma(\mu+i)}{\mathrm{t}}\right),\end{aligned} \tag{41}$$

$$\begin{aligned}\Phi_4 &= \left(\frac{q_k\mu_r}{B^r}\right)^{-\frac{\mu+i}{r}}\left(\frac{r\Gamma(\alpha-(\mu+i)r)}{(\xi^2-(\mu+i)r)(\mu+i)}\right. \\ &\left.\times\Gamma\left(t-(\mu+i)r\right)\left(\frac{\bar{\gamma}}{\mu(K+1)Q}\right)^{-\frac{\mu+i}{r}}\right),\end{aligned} \tag{42}$$

In addition, the diversity gain is given by

$$G_d=\min\left(\frac{\mu+i}{r},\frac{\zeta^2}{r},\frac{\alpha}{r},\frac{t}{r}\right). \tag{43}$$

2) DF Relaying: By substituting (29) into (36), and employing the similar method afore-mentioned, the closed-form

$$\bar{P}_e^{AF} = \frac{\delta}{2n} - \frac{\delta}{2\Gamma(p)} \frac{\zeta^2 A_1}{2^r} \sum_{t=1}^{\beta} b_t \sum_{i=0}^{\infty} \frac{w_i}{\Gamma(\mu+i)} \sum_{k=1}^{n} H_{1,0;2,0;4,2}^{0,1;0,2;0,4} \left[\begin{matrix} \left(1, -1, \frac{1}{r}\right) \\ - \\ (1;1), (1-\mu-i;1) \\ - \\ (1-\zeta^2,1), (1-\alpha,1), (1-t,1), (1-p,-\frac{1}{r}) \\ \left(0, \frac{1}{r}\right), \left(-\zeta^2, 1\right) \end{matrix} \middle| \begin{matrix} \\ \\ \\ \\ \\ \\ \frac{\bar{\gamma}}{\mu(K+1)Q}, \frac{1}{B}\left(q_k \mu_r\right)^{\frac{1}{r}} \end{matrix} \right], \tag{37}$$

formulation can be expressed as

$$\bar{P}_e^{DF} = \frac{n\delta}{2} - \frac{\delta}{2\Gamma(p)} \frac{\zeta^2 A_1 r}{2^r} \sum_{t=1}^{\beta} b_t \sum_{i=0}^{\infty} \frac{w_i}{\Gamma(\mu+i)} H_{1,0;1,2;2,4}^{0,1;2,0;4,0} \left[\begin{matrix} (1-p;1,1) \\ - \\ (1,1) \\ (0,1)\,(\mu+i,1) \\ (\zeta^2+1,r), (1,1) \\ (0,1), (\zeta^2,r), (\alpha,r), (t,r) \end{matrix} \middle| \begin{matrix} \\ \\ \\ \\ \\ \\ \frac{\mu(K+1)}{\bar{\gamma} q_k} \frac{B^r}{\mu_r q_k} \end{matrix} \right], \tag{44}$$

By inserting (30) into the average BER (36), and performing some algebraic manipulation, the asymptotic expression with DF scheme is derived as

$$\begin{aligned} \bar{P}_e^{DF\infty} \approx\ & \frac{\delta}{2\Gamma(p)} \sum_{k=1}^{n} \frac{\zeta^2 A_1 r}{2^r} \sum_{t=1}^{\beta} b_t \sum_{j=1}^{3} \Xi_j \Gamma\left(p+\phi_j\right) \\ & + \frac{\delta}{2\Gamma(p)} \sum_{k=1}^{n} \sum_{i=0}^{\infty} \frac{w_i}{\Gamma(\mu+i)(\mu+i)} \\ & \times \left(\frac{\mu(K+1)}{\bar{\gamma} q_k}\right)^{\mu+i} \Gamma\left(p+(\mu+i)\right) \end{aligned}, \tag{45}$$

where $\phi_{j=1}^{3} = \left\{\frac{\zeta^2}{r}, \frac{\alpha}{r}, \frac{t}{r}\right\}$

$$\Xi_1 = \left(\frac{\Gamma(\alpha-\zeta^2)\Gamma(t-\zeta^2)}{\zeta^2} \left(\frac{B^r}{\mu_r q_k}\right)^{\frac{\zeta^2}{r}}\right) \Gamma\left(p+\frac{\zeta^2}{r}\right), \tag{46}$$

$$\Xi_2 = \left(\frac{1}{\alpha(\zeta^2-\alpha)} \Gamma\left(t-\alpha\right) \left(\frac{B^r}{\mu_r q_k}\right)^{\frac{\alpha}{r}}\right) \Gamma\left(p+\frac{\alpha}{r}\right), \tag{47}$$

$$\Xi_3 = \left(\frac{1}{t(\zeta^2-t)} \Gamma\left(\alpha-t\right) \left(\frac{B^r}{\mu_r q_k}\right)^{\frac{t}{r}}\right) \Gamma\left(p+\frac{t}{r}\right), \tag{48}$$

Furthermore, the diversity gain is given by

$$G_d = \min\left(\frac{\zeta^2}{r}, \frac{\alpha}{r}, \frac{t}{r}\right). \tag{49}$$

C. Ergodic Capacity

The EC which represents the maximum date rate when error probability tends to be infinitely small, can be provided by

$$\bar{C} = \mathbb{E}\left[\log_2\left(1+n\gamma\right)\right], \tag{50}$$

where n represents a constant numerical value related to the detection methods. The system employs the HD ($r=1$) and IM/DD ($r=2$) technique when $n=1$ and $n=e/2\pi$, respectively. Besides, we can rewrite the EC with the CCDF of γ as

$$\bar{C} = \frac{n}{\ln(2)} \int_0^{\infty} \frac{F_{\gamma}^{c}(\gamma)}{1+n\gamma} d\gamma, \tag{51}$$

1) AF Relaying: The EC of mixed FSO/MMW system with various detection techniques under AF relaying can be formulated as (52) at the top of next page.

Proof: Inserting the CCDF of (20) into (51), the simplified expression with integration form (53) is derived at the top of next page. By utilizing [34, Eq. (4.293.10)], the EC can be provided by

$$\begin{aligned} \bar{C}^{AF} =\ & \frac{1}{\ln(2)} \frac{\zeta^2 A_1}{2^r} \sum_{t=1}^{\beta} b_t \sum_{i=0}^{\infty} \frac{w_i}{\Gamma(\mu+i)} \\ & \times \left(\frac{1}{2\pi i}\right)^2 \int_{L_1} \int_{L_2} \Gamma\left(-\tau_2+\frac{\tau_1}{r}\right) \Gamma\left(1-\frac{\tau_1}{r}\right) \Gamma\left(\frac{\tau_1}{r}\right) \\ & \times \frac{\Gamma\left(\zeta^2+\tau_1\right)\Gamma(\alpha+\tau_1)\Gamma(t+\tau_1)}{\Gamma\left(1+\frac{\tau_1}{r}\right)\Gamma(\zeta^2+1+\tau_1)} \left(B\left(\frac{1}{n\mu_r}\right)^{\frac{1}{r}}\right)^{-\tau_1} \\ & \times \Gamma\left(\tau_2\right) \Gamma\left(\mu+i+\tau_2\right) \left(\frac{\mu(K+1)Q}{\bar{\gamma}}\right)^{-\tau_2} d\tau_1 d\tau_2 \end{aligned}. \tag{54}$$

The proof is completed after some mathematical manipulations with [45, Eq. (1.1)]. ■

For $\rho=1, \Omega'=1$ and $\mu=1$, the EC in (52) simplifies to [46, Eq. (37)]. Furthermore, when we set $\Delta=0, \rho=1, \Omega'=1$ and $\mu=1$, the EC in (54) of the mixed FSO/MMW system converts to the special case where the S-R link experiences GG distribution as well as the R-D link follows FTR fading.

2) DF Relaying: By using $\frac{1}{1+n\gamma} = H_{1,1}^{1,1}\left[n\gamma \middle| \begin{matrix}(0,1)\\(0,1)\end{matrix}\right]$ [35, Eq. (1.43)] and substituting the CCDF of (29) into (51), the integration form of EC with DF relaying can be derived as

$$\begin{aligned} \bar{C}^{DF} =\ & \frac{n}{\ln(2)} \frac{\zeta^2 A_1 r}{2^r} \sum_{t=1}^{\beta} b_t \sum_{i=0}^{\infty} \frac{w_i}{\Gamma(\mu+i)} \\ & \times \int_0^{\infty} H_{1,1}^{1,1}\left[n\gamma \middle| \begin{matrix}(0,1)\\(0,1)\end{matrix}\right] \\ & \times H_{2,4}^{4,0}\left[\frac{B^r\gamma}{\mu_r} \middle| \begin{matrix}(\zeta^2+1,r),(1,1)\\(0,1),(\zeta^2,r),(\alpha,r),(t,r)\end{matrix}\right] \\ & \times H_{1,2}^{2,0}\left[\frac{\mu(K+1)\gamma}{\bar{\gamma}} \middle| \begin{matrix}(1,1)\\(0,1)\,(\mu+i,1)\end{matrix}\right] d\gamma \end{aligned}, \tag{55}$$

By utilizing the identity presented in [45, Eq. (2.3)], the integration form can be expressed as (56) shown on the top of next page.

D. Effective Capacity

Another important metric for the relaying system is EFC, which denotes the minimum delay and the efficient constant date-rate, can be given by

$$\begin{aligned} R &= -\tfrac{1}{A}\log_2\left(\mathbb{E}(1+\gamma)^{-A}\right) \\ &= -\tfrac{1}{A}\log_2\left(1 - A\int_0^{\infty}(1+\gamma)^{-A-1} F_{\gamma}^{C}(\gamma) d\gamma\right) \end{aligned}, \tag{57}$$

$$\bar{C}^{AF} = \frac{1}{\ln(2)} \frac{\zeta^2 A_1}{2^r} \sum_{t=1}^{\beta} b_t \sum_{i=0}^{\infty} \frac{w_i}{\Gamma(\mu+i)} H_{1,0;2,0;4,1}^{0,1;0,2;0,4} \times \left[\begin{array}{c} \left(1; -1, \frac{1}{r}\right) \\ - \\ (1;1), (1-\mu-i;1) \\ - \\ (1-\zeta^2,1)(1-\alpha,1)(1-t,1)\left(0-\frac{1}{r}\right)\left(1,\frac{1}{r}\right) \\ \left(0,\frac{1}{r}\right)\left(-\zeta^2,1\right) \end{array} \middle| \begin{array}{c} \\ \\ \\ \\ \\ \frac{\bar{\gamma}}{\mu(K+1)Q}, \frac{1}{B}(n\mu_r)^{\frac{1}{r}} \end{array} \right], \tag{52}$$

$$\bar{C}^{AF} = \frac{n}{\ln(2)} \frac{\zeta^2 A_1}{2^r} \sum_{t=1}^{\beta} b_t \sum_{i=0}^{\infty} \frac{w_i}{\Gamma(\mu+i)} \left(\frac{1}{2\pi i}\right)^2 \int_{L_1}\int_{L_2} \Gamma\left(-\tau_2 + \frac{\tau_1}{r}\right) \frac{\Gamma\left(\zeta^2+\tau_1\right)\Gamma(\alpha+\tau_1)\Gamma(t+\tau_1)}{\Gamma\left(1+\frac{s_1}{r}\right)\Gamma(\zeta^2+1+\tau_1)} \left(B\left(\frac{1}{\mu_r}\right)^{\frac{1}{r}}\right)^{-\tau_1} \times \Gamma(\tau_2)\Gamma(\mu+i+\tau_2)\left(\frac{\mu(K+1)Q}{\bar{\gamma}}\right)^{-\tau_2} d\tau_1 d\tau_2 \int_0^{\infty} \frac{\gamma^{-\frac{s_1}{r}}}{1+n\gamma} d\gamma, \tag{53}$$

$$\bar{C}^{DF} = \frac{n}{\ln(2)} \frac{\zeta^2 A_1 r}{2^r} \sum_{t=1}^{\beta} b_t \sum_{i=0}^{\infty} \frac{w_i}{\Gamma(\mu+i)} \frac{\bar{\gamma}}{\mu(K+1)} H_{2,1;1,1;2,4}^{0,2;1,1;4,0} \left[\begin{array}{c} (0;1,1)\,(-\mu-i;1,1) \\ (-1;1,1) \\ (0,1) \\ (0,1) \\ (\zeta^2+1,r),(1,1) \\ (0,1),(\zeta^2,r),(\alpha,r),(t,r) \end{array} \middle| \begin{array}{c} \\ \\ \\ \\ \\ \frac{\bar{\gamma}c}{\mu(K+1)}, \frac{\bar{\gamma}B^r}{\mu(K+1)\mu_r} \end{array} \right]. \tag{56}$$

where $A = \frac{\theta T B_R}{\ln 2}$. T represents the length of block., θ represents the rate at which the buffer occupancy diminishes asymptotically and B_R is system bandwidth [46].

1) AF Relaying: The EFC of S-D link SNR with AF scheme is given by (58) shown on the top of the next page.

Proof: By applying (20) into (57) and utilizing [34, Eq. (3.194.3)], the EFC can be derived as

$$R^{AF} = -\frac{1}{A}\log_2 \left(1 - \frac{\zeta^2 A_1 A}{2^r} \sum_{t=1}^{\beta} b_t \sum_{i=0}^{\infty} \frac{w_i}{\Gamma(\mu+i)\Gamma(1+A)} \times \left(\frac{1}{2\pi i}\right)^2 \int_{L_1}\int_{L_2} \Gamma\left(-\tau_2 + \frac{\tau_1}{r}\right)\Gamma\left(1-\frac{\tau_1}{r}\right)\Gamma\left(A+\frac{\tau_1}{r}\right) \times \frac{\Gamma\left(\zeta^2+\tau_1\right)\Gamma(\alpha+\tau_1)\Gamma(t+\tau_1)}{\Gamma\left(1+\frac{\tau_1}{r}\right)\Gamma(\xi^2+1+\tau_1)} \left(B\left(\frac{1}{\mu_r}\right)^{\frac{1}{r}}\right)^{-\tau_1} \times \Gamma(\tau_2)\Gamma(\mu+i+\tau_2)\left(\frac{\mu(K+1)Q}{\bar{\gamma}}\right)^{-\tau_2} d\tau_1 d\tau_2\right). \tag{59}$$

Using [45, Eq. (1.1)], the proof is completed. ■

Note that when $\rho = 1, \Omega' = 1$ and $\mu = 1$, the EFC in (58) can reduce to [46, Eq. (40)].

2) DF Relaying: Inserting (29) into (57) with [45, Eq. (2.3)], and utilizing $(1+\gamma)^{-A-1} = H_{1,1}^{1,1}\left[\gamma \middle| \begin{array}{c} (-A,1) \\ (0,1) \end{array}\right]$ [35, Eq. (1.43)], we can use the Fox's-H function to rewrite the EFC of the FSO/MMW system with DF relaying as (60) at the top of next page.

Specially, setting $\rho = 1, \Omega' = 1$ and $\mu = 1$, (60) can be reduced to [46, Eq. (46)].

V. Numerical Results

Numerical results are provided to verify the effect of variable key parameters of the satellite-terrestrial relay system in this section. Analytical formulae are validated for their accuracy by MC simulations in the MATLAB. We presume that the average SNR values for different links obey $\bar{\gamma}_{FSO} = \bar{\gamma}_{RF} = \bar{\gamma}$ in these figures. The turbulence parameters of Málaga ($\mathcal{M}$) distribution encompass ($\alpha = 2.296, \beta = 2$) and ($\alpha = 4.2, \beta = 3$) [21], which are set for strong and moderate turbulence of the $S-R$ link. The value for $\zeta = 1.1$ and $\zeta = 6.7$ represents strong and negligible pointing error, respectively, and $\bar{\gamma}_{th}$ is set to a constant value of 10 dB. The values of relevant system parameters and weather-dependent variables for the FSO and RF subsystems are extracted from [39], [40], [47], [48] and tabulated in Table IV.

TABLE IV: Parameters of FSO and RF sub-systems

Parameter	Symbol	Value
FSO System		
light speed	C	$3 \times 10^5 km/s$
Optical power	P_{FSO}	$4dB$
Receive gain	G_R	$45dB$
Maximal satellite beam gain	G_{max}	$53dB$
Carrier frequency	f_{FSO}	$2GHz$
Distence between $S-R$	d_{SR}	$35786km$
Receiver noise temperature	T	$300K$
3dB angle	φ_{3dB}	0.4°
RF System		
Transmit antenna gain	G_t	$43dBi$
Receive antenna gain	G_r	$43dBi$
Transmit power	P_{RF}	$10mW$
Attenuation(Oxygen)	a_{oxy}	$15.1dB/km$
Attenuation(Rain)	a_{rain}	$0dB/km$
Noise power spectral density	$N_{0_{RF}}$	$-114dBm/MHz$
Receiver noise figure	N_{RF}	$5dB$
Distence between $R-D$	d_{RD}	$1.5km$
Carrier frequency	f_{RF}	$60GHz$
Bandwidth	B_{RF}	$250MHz$

In Fig. 2, the effects of the strong and moderate atmospheric turbulence on the OP performance are depicted. The mixed satellite-terrestrial FSO/MMW system employs strong and negligible pointing errors over the HD ($r = 1$). The relay is assumed to use fixed-gain AF with fixed $Q = 1.7$ and γ_{th} = 10 dB. Meanwhile, the RF link follows MFTR fading distribution ($K = 15, m = 5, \Delta = 0.1$). It is evident that the points of

$$R^{AF} = -\frac{1}{A}\log_2\left(1 - \frac{\zeta^2 A_1 A}{2^r}\sum_{t=1}^{\beta} b_t \sum_{i=0}^{\infty} \frac{w_i}{\Gamma(\mu+i)\Gamma(1+A)} H_{1,0;2,0;5,2}^{0,1;0,2;0,5}\left[\begin{array}{c} (1;-1,\frac{1}{r}) \\ - \\ (1;1),(1-\mu-i;1) \\ - \\ (1-\zeta^2,1),(1-\alpha,1),(1-t,1),(0,-\frac{1}{r}),(1-A,\frac{1}{r}) \\ (0,\frac{1}{r}),(-\zeta^2,1) \end{array}\middle| \frac{\bar{\gamma}}{\mu(K+1)}\frac{1}{B}(\mu_r)^{\frac{1}{r}}\right]\right), \tag{58}$$

$$R^{DF} = -\frac{1}{A}\log_2\left(1 - \frac{\zeta^2 A_1 A}{2^r}\sum_{t=1}^{\beta} b_t \sum_{i=0}^{\infty} \frac{w_i}{\Gamma(\mu+i)\Gamma(1+A)} H_{2,0;2,1;4,2}^{0,2;0,2;0,4}\left[\begin{array}{c} (0;\frac{1}{r},1),(1-A;-\frac{1}{r},-1) \\ - \\ (1,1),(1-\mu-i,1) \\ (0,1) \\ (1-\zeta^2,1),(1-\alpha,1),(1-t,1),(1,\frac{1}{r}) \\ (0,\frac{1}{r}),(-\zeta^2,1) \end{array}\middle| \frac{\bar{\gamma}}{\mu(K+1)}\frac{1}{B}(\mu_r)^{\frac{1}{r}}\right]\right), \tag{60}$$

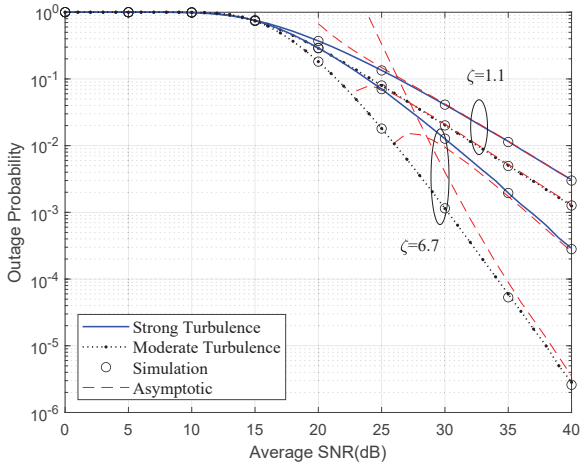

Fig. 2: OP v.s. average SNR for varying pointing errors of a mixed FSO/MMW model, considering fixed-gain AF relay and the HD technique, under various turbulence scenarios ($K = 15, m = 5, \Delta = 0.1$ and $\mu = 2$).

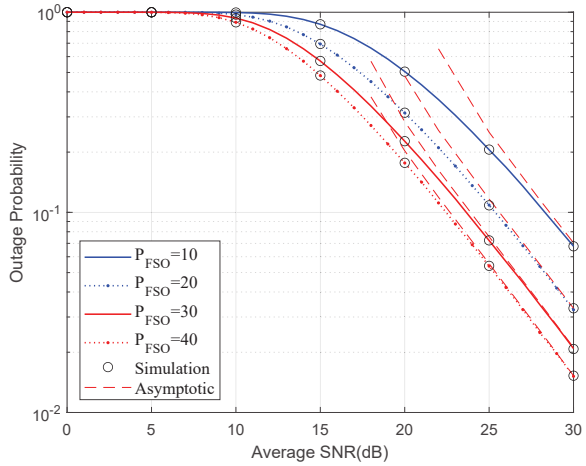

Fig. 3: OP v.s. average SNR for varying optical power of a mixed FSO/MMW model, considering fixed-gain AF relay and the HD technique, under various turbulence scenarios ($K = 15, m = 5, \Delta = 0.1$ and $\mu = 2$).

the analytical curves fit well with the MATLAB simulation curves. As expected, the OP decreases substantially with $\zeta = 6.7$, which represents negligible point error impairments. Moreover, the atmospheric turbulence parameters α and β influence the performance of OP significantly. The turbulence parameters will decrease in the worse environment conditions. The numerical results also demonstrate that the asymptotic expression in (21) shows a comparable decline rate in the outage curves under high SNR conditions. The numerical results in (20) can be confirmed to closely match the average SNR MC simulations with AF scheme.

The figure presented in Fig. 3 illustrates the influence of varying optical power levels on the OP of the analyzed system with $P_{RF} = 10dB$ under AF relay. As anticipated, optical power manifests a positive impact. Optical power undeniably enhances the received SNR, leading to an unequivocal improvement in outage performance. However, it is noteworthy that as the optical power increases, there is a gradual deceleration in the rate of improvement in the performance.

We assume DF relaying and the HD technique with fixed values of $K = 15, m = 5, \Delta = 0.1, \alpha = 2.296, \beta = 2$ and $\mu = 2$ to compare the average BER for DBPSK ($p = 1, q_k = 1, \delta = 1, n = 1$) and CBPSK ($p = 0.5, q_k = 1, \delta = 1, n = 1$) under variable pointing errors in Fig.4. Obviously, the average BER for both modulation schemes decreases along with the increase of average BER under different pointing error conditions. Also, CBPSK performs better than DBPSK and negligible pointing errors improves the average BER performance more visibly than strong pointing error. In addition, the asymptotic results match tightly with the exact counterpart at high SNR. Meanwhile, the exact mathematical results of average BER and the MC simulations have a low error margin. It can be confirmed that the analytical results and the MC curves match closely.

The average BER with variable detection techniques in DBPSK ($p = 1, q_k = 1, \delta = 1, n = 1$) is depicted in Fig.

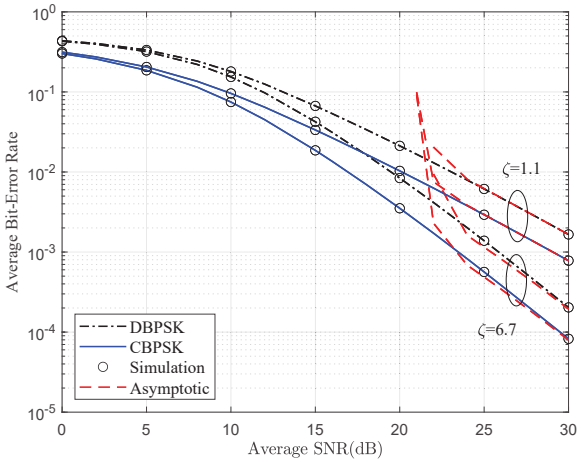

Fig. 4: Average BER v.s. average SNR for variable pointing error of a mixed FSO/MMW model with DF scheme and the HD technique for CBPSK and DBPSK modulation conditions ($K = 15, m = 5, \Delta = 0.1, \alpha = 2.296, \beta = 2$ and $\mu = 2$).

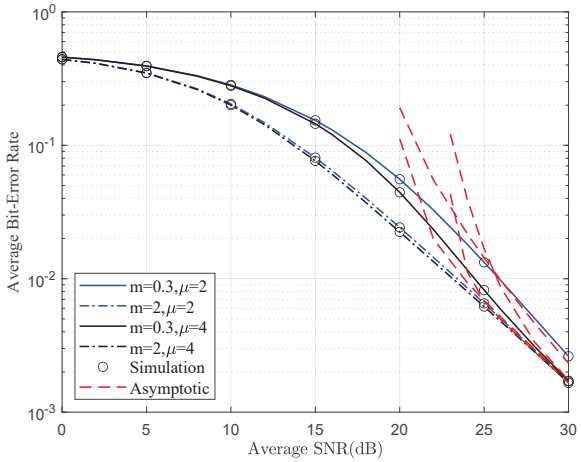

Fig. 6: Average BER v.s. average SNR for variable fading severity parameters, m, of a mixed FSO/MMW model with DF scheme and DBPSK modulation for varying numbers of clusters ($K = 10, \Delta = 0.5, \mu = 2, \alpha = 2.296, \beta = 2$ and $\zeta = 1.1$).

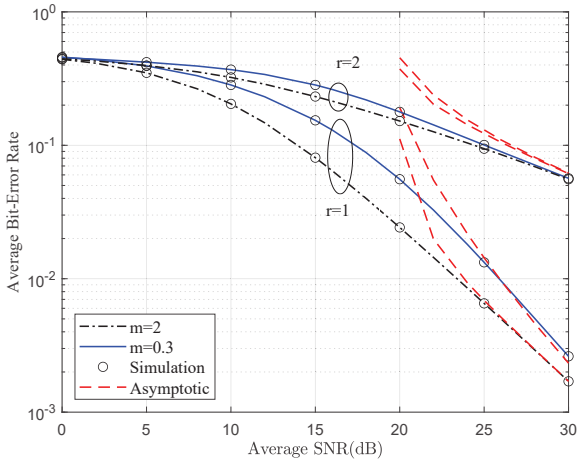

Fig. 5: Average BER v.s. average SNR for variable fading severity parameters, m, of a mixed FSO/MMW model with DF relaying and DBPSK modulation under variable detection ($K = 10, \Delta = 0.5, \mu = 2, \alpha = 2.296, \beta = 2$ and $\zeta = 1.1$).

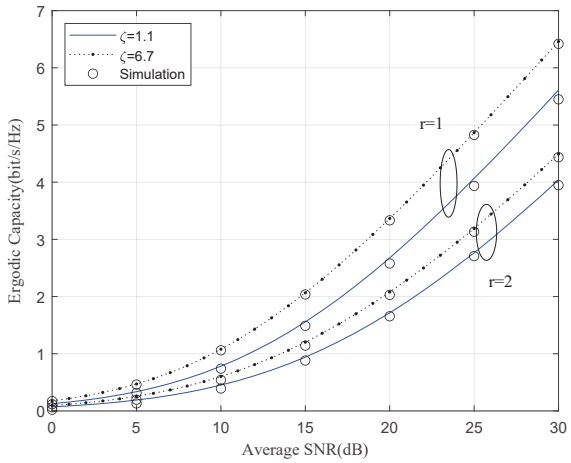

Fig. 7: EC v.s. average SNR for variable pointing error impairments of a mixed FSO/MMW model with DF scheme for both HD and IM/DD detection conditions ($K = 15, m = 5, \Delta = 0.1, \mu = 2, \alpha = 2.296$ and $\beta = 2$).

5, which assumes $K = 10, \Delta = 0.5, \mu = 2, \alpha = 2.296, \beta = 2$ and $\zeta = 1.1$. It can be concluded that the improvement of the average BER performance with the IM/DD technique is less than in the the HD technique. Obviously, the average BER performs better under low fading severe parameter ($m = 0.3$) for the relay system. It is straightforward to observe that the gap between curves with different fading parameters under the same detection technique becomes negligible at high SNR. This implies that the impact of the severe fading parameter m on detection techniques r, especially in the case of $r = 2$, is not significant. Moreover, the analytical accuracy is verified by the MC simulations.

Fig. 6 plots the $m = 0.3$ and $m = 2$ curves of average BER under the DF relay system, which illustrates the effect of the number of clusters with fixed parameters $K = 10, \Delta = 0.5, \mu = 2, \alpha = 2.296, \beta = 2$ and $\zeta = 1.1$. It is worth noting that the average BER performs better with more clusters ($\mu = 4$). As depicted in the curves, the analytical results fit well with the MC simulation, as well as asymptotic results at high SNRs. It is noteworthy that when $m = 2$, the number of clusters μ shows minimal impact on the average BER improvement. Moreover, it is evident that the gap between the curves decreases, suggesting that the average BER is less impacted by the number of clusters μ.

In Fig. 7, $K = 15, m = 5, \Delta = 0.1, \mu = 2, \alpha = 2.296$ and $\beta = 2$ are fixed. The EC of the DF relay under variable detection techniques for different pointing errors is presented. The simulation results validate the accuracy. It is worth noting that the HD technique is better than the IM/DD technique in EC performance with varying pointing errors. Meanwhile, IM/DD has a more significant impact on pointing errors. Furthermore, our analysis is validated by the close agreement between the MC simulations and the theoretical results.

In Fig. 8, we consider the case $K = 15, m = 5, \Delta =$

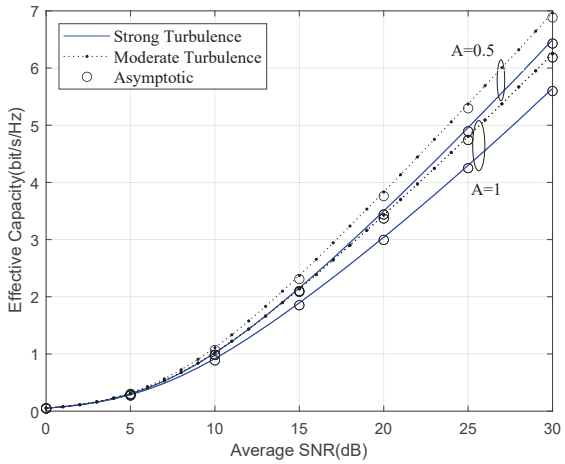

Fig. 8: EFC v.s. average SNR for variable turbulence impairments of a mixed FSO/MMW model with AF scheme and the HD for variable A conditions ($K = 15, m = 5, \Delta = 0.1, \mu = 2$ and $\zeta = 1.1$).

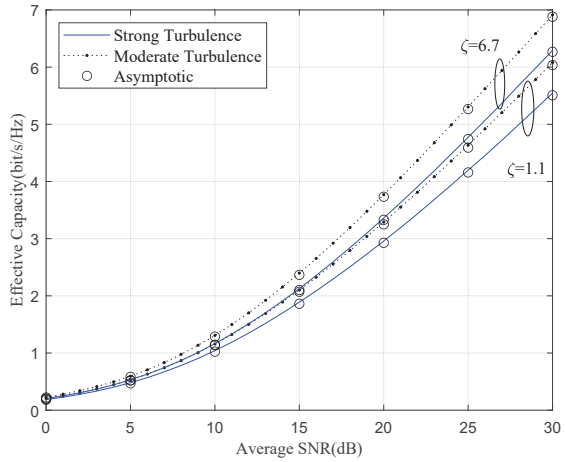

Fig. 9: EFC v.s. average SNR for variable turbulence impairments of a mixed FSO/MMW model with DF relaying and the HD technique under variable pointing error conditions ($K = 15, m = 5, \Delta = 0.1, \mu = 2$ and $A = 1$).

$0.1, \mu = 2$ and $\zeta = 1.1$. The theoretical and simulation results of EFC in satellite-terrestrial relaying systems employ various turbulence degrees with different A. As expected, the EFC increases along with the average SNR under different turbulence parameters and the moderate turbulence performs better. It is straightforward to see that the figure results are fit well with the simulation curves.

We assume $K = 15, m = 5, \Delta = 0.1, \mu = 2$, and $A = 1$ in Fig. 9, which demonstrates the EFC of the FSO/MMW system of various pointing error impairments under strong and moderate turbulence with the HD technique ($r = 1$). A clear improvement of EFC with average SNR increase under different degrees of turbulence is observed. It is evident that the EFC is vulnerable to the turbulence and a substantial improvement is anticipated for the negligible pointing error impairments ($\zeta = 6.7$). Besides, the results of the MC simulations in MATLAB are validate the analytical counterparts.

Fig. 10 demonstrates the OP of FSO/MMW systems using variable gain AF, fixed-AF, and DF relaying under the HD technique. In this figure, we compare the OP of variable gain AF relaying, fixed-gain AF relaying and DF relaying. It can be observed that fixed-gain AF relaying exhibits the best OP performance. Furthermore, it is evident that the gap between the curves decreases. Since the relay system is primarily influenced by the FSO channel, the RF channel parameters have a relatively minor impact on the system performance.

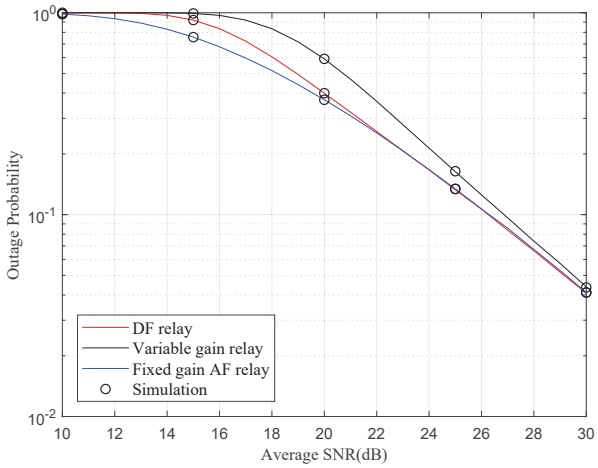

Fig. 10: OP of FSO/MMW systems using variable gain AF, fixed-AF, and DF relaying under the HD technique. ($\alpha = 2.296, \beta = 2, \zeta = 1.1, K = 15, m = 5, \Delta = 0.1$ and $\mu = 2$).

VI. Conclusion

In this work, new closed-form expressions of a satellite-terrestrial FSO/MMW relaying systems have been derived with Málaga ($\mathcal{M}$) distribution and MFTR fading, respectively. Furthermore, employing fixed-gain AF and DF relays, the closed-form performance expressions of end-to-end link with both detection techniques for the OP, average BER, EC and EFC have been demonstrated with bivariate Fox's-H function. Additionally, we have provided the asymptotic results at high SNRs as well as derived the diversity orders. The simulation results have validated the provided analytical results and emphasized the significant consequences of the turbulence parameter, pointing error, detection method, the MFTR fading parameters and the number of clusters for end-to-end transmission. On this foundation, the performance of the relay system is primarily influenced by the FSO channel parameters, and the RF channel parameters have a relatively minor impact on system performance. As expected, the system performance can be significantly improved in the case of negligible atmospheric turbulence, weak pointing errors, HD technique, and increase of the fading parameters, while the presence of multi-path clusters has a negligible effect.

APPENDIX A
PROOF OF CDF OF SNR FOR AF RELAYING

By deriving the CDF of S-D link SNR γ^{AF}, we obtain

$$\begin{aligned} &F_{\gamma^{AF}}^{S-D}(\gamma) = \Pr(\gamma_{AF} < \gamma) \\ &= \Pr\left(\frac{\gamma_{FSO}\gamma_{RF}}{\gamma_{RF}+Q} < \gamma\right) \\ &= 1 - \int_0^{\infty} f_{\gamma_{FSO}}(x+\gamma)\left[1 - F_{\gamma_{RF}}\left(\frac{Q\gamma}{x}\right)\right] dx \end{aligned} , \quad (A.1)$$

By substituting (6), (17) into (A.1) and applying the formulation [34, Eq. (9.301)] which relates to the Meijer's G-function, then (A.1) can be rewritten as

$$\begin{aligned} &F_{\gamma^{AF}}^{S-D}(\gamma) = 1 - \frac{\zeta^2 A_1}{2^r}\sum_{t=1}^{\beta} b_t \sum_{i=0}^{\infty}\frac{w_i}{\Gamma(\mu+i)}\frac{1}{2\pi i} \\ &\times \int_{L_1} \frac{\Gamma\left(\zeta^2-\tau_1\right)\Gamma(\alpha-\tau_1)\Gamma(t-\tau_1)}{\Gamma(\zeta^2+1-\tau_1)}\left(B\left(\frac{1}{\mu_r}\right)^{\frac{1}{r}}\right)^{\tau_1} d\tau_1 \\ &\times \frac{1}{2\pi i}\int_{L_2} \frac{\Gamma(-\tau_2)\Gamma(\mu+i-\tau_2)}{\Gamma(1-\tau_2)}\left(\frac{\mu(K+1)Q\gamma}{\bar{\gamma}}\right)^{\tau_2} d\tau_2 \\ &\times \int_0^{\infty}\frac{(x+\gamma)^{\frac{\tau_1}{r}}}{x+\gamma} x^{-\tau_2} dx \end{aligned} , \quad (A.2)$$

where L_1 and L_2 denote the contours of τ_1-plane and τ_2-plane, respectively. Simplifying (A.2) with [34, Eq. (3.194.3), Eq. (8.384.1)], yields the following expression

$$\begin{aligned} &F_{\gamma^{AF}}^{S-D}(\gamma) = 1 - \frac{\zeta^2 A_1}{2^r}\sum_{t=1}^{\beta} b_t \sum_{i=0}^{\infty}\frac{w_i}{\Gamma(\mu+i)}\left(\frac{1}{2\pi i}\right)^2 \\ &\times \int_{L_1}\int_{L_2} \Gamma\left(-\tau_2+\frac{\tau_1}{r}\right)\Gamma(\tau_2)\Gamma(\mu+i+\tau_2) \\ &\times \frac{\Gamma\left(\zeta^2+\tau_1\right)\Gamma(\alpha+\tau_1)\Gamma(t+\tau_1)}{\Gamma\left(1+\frac{\tau_1}{r}\right)\Gamma(\zeta^2+1+\tau_1)} \\ &\times \left(B\left(\frac{\gamma}{\mu_r}\right)^{\frac{1}{r}}\right)^{-\tau_1}\left(\frac{\mu(K+1)Q}{\bar{\gamma}}\right)^{-\tau_2} d\tau_1 d\tau_2 \end{aligned} . \quad (A.3)$$

After some algebraic manipulations with the help of [45, Eq. (1.1)], we can obtain (20) with bivariate Fox's-H function to complete the proof.

APPENDIX B
PROOF OF ASYMPTOTIC CDF OF SNR FOR AF RELAYING

By employing the definition associated with the Fox's H-function [41, Eq. (1.1.2)] in (20), we have the asymptotic form of the CDF

$$\begin{aligned} &F_{\gamma^{AF}}^{\infty}(\gamma) \approx 1 - \frac{\zeta^2 A_1}{2\times 2^r}\sum_{t=1}^{\beta} b_t \sum_{i=0}^{\infty}\frac{w_i}{\Gamma(\mu+i)}\frac{1}{2\pi i} \\ &\times \int_{L_1} \frac{\Gamma\left(\zeta^2+\tau_1\right)\Gamma(\alpha+\tau_1)\Gamma(t+\tau_1)}{\Gamma\left(1+\frac{\tau_1}{r}\right)\Gamma(\zeta^2+1+\tau_1)}\left(B\left(\frac{\gamma}{\mu_r}\right)^{\frac{1}{r}}\right)^{-\tau_1} d\tau_1 \\ &\times H_{1,2}^{2,1}\left[\frac{\mu(K+1)Q}{\bar{\gamma}}\middle|\begin{matrix}\left(1-\frac{\tau_1}{r},1\right)\\(0,1),(\mu+i,1)\end{matrix}\right] \\ &-\frac{\zeta^2 A_1}{2\times 2^r}\sum_{t=1}^{\beta} b_t \sum_{i=0}^{\infty}\frac{w_i}{\Gamma(\mu+i)}\frac{1}{2\pi i} \\ &\times \int_{L_2} \Gamma(\tau_2)\Gamma(\mu+i+\tau_2)\left(\frac{\mu(K+1)Q}{\bar{\gamma}}\right)^{-\tau_2} d\tau_2 \\ &\times H_{2,4}^{4,0}\left[B\left(\frac{\gamma}{\mu_r}\right)^{\frac{1}{r}}\middle|\begin{matrix}\left(1,\frac{1}{r}\right),\left(\zeta^2+1,1\right)\\(-\tau_2,\frac{1}{r}),(\zeta^2,1),(\alpha,1),(t,1)\end{matrix}\right] \end{aligned} , \quad (B.1)$$

Moreover, with the utilization of [41, Th 1.7, Th 1.11], the asymptotic results with Fox's-H functions in (B.1) can be obtained

$$\begin{aligned} &H_{2,4}^{4,0}\left[B\left(\frac{\gamma}{\mu_r}\right)^{\frac{1}{r}}\middle|\begin{matrix}\left(1,\frac{1}{r}\right),\left(\zeta^2+1,1\right)\\(-\tau_2,\frac{1}{r}),(\zeta^2,1),(\alpha,1),(t,1)\end{matrix}\right] \\ &\approx r\frac{\Gamma\left(\zeta^2+\tau_2 r\right)\Gamma(\alpha+\tau_2 r)\Gamma(t+\tau_2 r)}{\Gamma(1+\tau_2)\Gamma(\zeta^2+1+\tau_2 r)}\left(B\left(\frac{\gamma}{\mu_r}\right)^{\frac{1}{r}}\right)^{-r\tau_2} \\ &+\frac{\Gamma\left(-\tau_2-\frac{\zeta^2}{r}\right)\Gamma\left(\alpha-\zeta^2\right)\Gamma\left(t-\zeta^2\right)}{\Gamma\left(1-\frac{\zeta^2}{r}\right)}\left(B\left(\frac{\gamma}{\mu_r}\right)^{\frac{1}{r}}\right)^{\zeta^2} \\ &+\frac{\Gamma\left(-\tau_2-\frac{\alpha}{r}\right)\Gamma\left(\zeta^2-\alpha\right)\Gamma(t-\alpha)}{\Gamma\left(1-\frac{\alpha}{r}\right)\Gamma(\zeta^2+1-\alpha)}\left(B\left(\frac{\gamma}{\mu_r}\right)^{\frac{1}{r}}\right)^{\alpha} \\ &+\frac{\Gamma\left(-\tau_2-\frac{t}{r}\right)\Gamma\left(\zeta^2-t\right)\Gamma(\alpha-t)}{\Gamma\left(1-\frac{t}{r}\right)\Gamma(\zeta^2+1-t)}\left(B\left(\frac{\gamma}{\mu_r}\right)^{\frac{1}{r}}\right)^{t} \end{aligned} , \quad (B.2)$$

and

$$\begin{aligned} &H_{1,2}^{2,1}\left[\frac{\mu(K+1)Q}{\bar{\gamma}}\middle|\begin{matrix}\left(1;-\frac{\tau_1}{r},1\right)\\(0,1),(\mu+i,1)\end{matrix}\right] \\ &\approx \Gamma(\mu+i)\Gamma\left(\frac{s_1}{r}\right) \\ &+\Gamma(-\mu-i)\Gamma\left(\frac{s_1}{r}+\mu+i\right)\left(\frac{\mu(K+1)Q}{\bar{\gamma}}\right)^{\mu+i} \end{aligned} . \quad (B.3)$$

After inserting (B.2) and (B.3) into (B.1) and performing necessary algebraic transformation, we can deduce (21) to complete the proof.

APPENDIX C
PROOF OF AVERAGE BER OF SNR FOR AF RELAYING

Inserting (20) into (36), we can obtain the average BER of AF relaying as

$$\begin{aligned} &\bar{P}_e^{AF} = \frac{n\delta}{2} - \frac{\delta}{2\Gamma(p)}\sum_{k=1}^{n} q_k^p \frac{\zeta^2 A_1}{2^r}\sum_{t=1}^{\beta} b_t \sum_{i=0}^{\infty}\frac{w_i}{\Gamma(\mu+i)} \\ &\times\left(\frac{1}{2\pi i}\right)^2 \int_{L_1}\int_{L_2} \frac{\Gamma\left(\zeta^2+\tau_1\right)\Gamma(\alpha+\tau_1)\Gamma(t+\tau_1)}{\Gamma\left(1+\frac{\tau_1}{r}\right)\Gamma(\zeta^2+1+\tau_1)} \\ &\times\Gamma\left(-\tau_2+\frac{\tau_1}{r}\right)\left(B\left(\frac{1}{\mu_r}\right)^{\frac{1}{r}}\right)^{-\tau_1} \\ &\times\Gamma(\tau_2)\Gamma(\mu+i+\tau_2)\left(\frac{\mu(K+1)Q}{\bar{\gamma}}\right)^{-\tau_2} d\tau_1 d\tau_2 \\ &\times\int_0^{\infty}\gamma^{p-1}\gamma^{-\frac{\tau_1}{r}}\exp(-q_k\gamma)d\gamma \end{aligned} , \quad (C.4)$$

Utilizing [34, Eq. (3.381.4)] into (C.5), we have the integral expressions as

$$\begin{aligned} &\bar{P}_e^{AF} = \frac{n\delta}{2} - \frac{\delta}{2\Gamma(p)}\frac{\zeta^2 A_1}{2^r}\sum_{t=1}^{\beta} b_t \sum_{i=0}^{\infty}\frac{w_i}{\Gamma(\mu+i)}\left(\frac{1}{2\pi i}\right)^2 \\ &\times \int_{L_1}\int_{L_2} \frac{\Gamma\left(\zeta^2+\tau_1\right)\Gamma(\alpha+\tau_1)\Gamma(t+\tau_1)\Gamma\left(p-\frac{\tau_1}{r}\right)}{\Gamma\left(1+\frac{\tau_1}{r}\right)\Gamma(\zeta^2+1+\tau_1)} \\ &\times\left(B\left(\frac{1}{q_k\mu_r}\right)^{\frac{1}{r}}\right)^{-\tau_1}\Gamma(\tau_2)\Gamma(\mu+i+\tau_2) \\ &\times\Gamma\left(-\tau_2+\frac{\tau_1}{r}\right)\left(\frac{\mu(K+1)Q}{\bar{\gamma}}\right)^{-\tau_2} d\tau_1 d\tau_2 \end{aligned} . \quad (C.5)$$

Using [45, Eq. (1.1)], then (37) is obtained, which completes the proof.

REFERENCES

[1] M. Dohler, R. W. Heath, A. Lozano, C. B. Papadias, and R. A. Valenzuela, "Is the PHY layer dead?" *IEEE Commun. Mag.*, vol. 49, no. 4, pp. 159–165, 2011.

[2] Z. Jia, M. Sheng, J. Li, D. Zhou, and Z. Han, "VNF-based service provision in software defined LEO satellite networks," *IEEE Trans. Wireless Commun. number=9, pages=6139–6153, year=2021, publisher=IEEE.*

[3] ——, "Joint HAP access and LEO satellite backhaul in 6G: Matching game-based approaches," *IEEE J. Sel. Areas Commun.*, vol. 39, no. 4, pp. 1147–1159, 2020.

[4] K. Guo, K. An, B. Zhang, Y. Huang, D. Guo, G. Zheng, and S. Chatzinotas, "On the performance of the uplink satellite multiterrestrial relay networks with hardware impairments and interference," *IEEE syst. J.*, vol. 13, no. 3, pp. 2297–2308, 2019.

[5] K. Guo, X. Li, M. Alazab, R. H. Jhaveri, and K. An, "Integrated satellite multiple two-way relay networks: Secrecy performance under multiple eves and vehicles with non-ideal hardware," *IEEE Trans. Intell. Veh.*, vol. 8, no. 2, pp. 1307–1318, 2022.

[6] A. Guidotti, A. Vanelli-Coralli, M. Conti, S. Andrenacci, S. Chatzinotas, N. Maturo, B. Evans, A. Awoseyila, A. Ugolini, T. Foggi *et al.*, "Architectures and key technical challenges for 5G systems incorporating satellites," *IEEE Trans. Veh. Technol.*, vol. 68, no. 3, pp. 2624–2639, 2019.

[7] E. Lagunas, S. K. Sharma, S. Maleki, S. Chatzinotas, and B. Ottersten, "Resource allocation for cognitive satellite communications with incumbent terrestrial networks," *IEEE Trans. Cogn. Commun. Netw.*, vol. 1, no. 3, pp. 305–317, 2015.

[8] J. Liu, Y. Shi, Z. M. Fadlullah, and N. Kato, "Space-air-ground integrated network: A survey," *IEEE Commun. Surv. Tut.*, vol. 20, no. 4, pp. 2714–2741, 2018.

[9] A. S. Hamza, J. S. Deogun, and D. R. Alexander, "Classification framework for free space optical communication links and systems," *IEEE Commun. Surveys Tuts.*, vol. 21, no. 2, pp. 1346–1382, 2019.

[10] J. Laneman, D. Tse, and G. Wornell, "Cooperative diversity in wireless networks: Efficient protocols and outage behavior," *IEEE Trans. Inf. Theory*, vol. 50, no. 12, pp. 3062–3080, 2004.

[11] J. D. V. Sánchez, F. J. López-Martínez, J. F. Paris, and J. M. Romero-Jerez, "The multi-cluster fluctuating two-ray fading model," *arXiv preprint arXiv:2212.02448*, 2022.

[12] H. Du, J. Zhang, K. Guan, D. Niyato, H. Jiao, Z. Wang, and T. Kürner, "Performance and optimization of reconfigurable intelligent surface aided THz communications," *IEEE Trans. Commun.*, vol. 70, no. 5, pp. 3575–3593, 2022.

[13] J. M. Romero-Jerez, F. J. Lopez-Martinez, J. P. Peña-Martín, and A. Abdi, "Stochastic fading channel models with multiple dominant specular components," *IEEE Trans. Veh. Technol.*, vol. 71, no. 3, pp. 2229–2239, 2022.

[14] Z. Zhao, G. Xu, N. Zhang, and Q. Zhang, "Symbol error analysis of amplify-and-forward based multiuser hybrid satellite-terrestrial relay network," *IEEE Wireless Commun. Lett.*, vol. 10, no. 10, pp. 2279–2283, 2021.

[15] L. Kong, W. Xu, L. Hanzo, H. Zhang, and C. Zhao, "Performance of a free-space-optical relay-assisted hybrid RF/FSO system in generalized M-distributed channels," *IEEE Photonics J.*, vol. 7, no. 5, pp. 1–19, 2015.

[16] J. Ding, X. Xie, L. Tan, J. Ma, and D. Kang, "Dual-hop RF/FSO systems over κ-μ shadowed and fisher-snedecor $\mathcal{F}$ fading channels with non-zero boresight pointing errors," *J. Light. Technol.*, vol. 40, no. 3, pp. 708–719, 2022.

[17] N. H. Juel, A. S. M. Badrudduza, S. M. R. Islam, S. H. Islam, M. K. Kundu, I. S. Ansari, M. M. Mowla, and K.-S. Kwak, "Secrecy performance analysis of mixed $\alpha-\mu$ and exponentiated weibull RF/FSO cooperative relaying system," *IEEE Access*, vol. 9, pp. 72 342–72 356, 2021.

[18] Z. Wang, W. Shi, and W. Liu, "Performance analysis of mixed RF/FSO system with spatial diversity," *Opt. Commun.*, vol. 443, pp. 230–237, 2019.

[19] S. Li, Y. Yang, L. Yang, and Y. Bian, "On the study of multiuser mixed dual-hop RF/THz systems," *IEEE Trans. Veh. Technol.*, pp. 1–14, 2023.

[20] I. Trigui, S. Affes, A. M. Salhab, and M.-S. Alouini, "Multi-user mixed FSO/RF systems with aperture selection under poisson field interference," *IEEE Access*, vol. 7, pp. 73 764–73 781, 2019.

[21] J. Hu, Z. Zhang, J. Dang, L. Wu, and G. Zhu, "Performance of decode-and-forward relaying in mixed beaulieu-xie and $\mathcal{M}$ dual-hop transmission systems with digital coherent detection," *IEEE Access*, vol. 7, pp. 138 757–138 770, 2019.

[22] P. Sarma, R. Deka, and S. Anees, "Performance analysis of DF based mixed triple hop RF-FSO-UWOC cooperative system," in *IEEE 92nd Veh. Technol. Conf. (VTC-Fall)*. IEEE, 2020, pp. 1–5.

[23] E. Balti and M. Guizani, "Mixed RF/FSO cooperative relaying systems with co-channel interference," *IEEE Trans. Commun.*, vol. 66, no. 9, pp. 4014–4027, 2018.

[24] S. Sharma, A. S. Madhukumar, and R. Swaminathan, "Effect of pointing errors on the performance of hybrid FSO/RF networks," *IEEE Access*, vol. 7, pp. 131 418–131 434, 2019.

[25] H. A. Siddig, A. M. Salhab, and S. A. Zummo, "Performance analysis and optimization of multiuser mixed FSO/RF cognitive radio DF relay network," *Arab. J. Sci. Eng.*, vol. 47, no. 3, pp. 3649–3657, 2022.

[26] M. A. Amirabadi and V. T. Vakili, "Performance of a relay-assisted hybrid FSO/RF communication system," *Phys. commun.*, vol. 35, p. 100729, 2019.

[27] Z. Zhang, Q. Sun, M. López-Benítez, X. Chen, and J. Zhang, "Performance analysis of dual-hop RF/FSO relaying systems with imperfect CSI," *IEEE Trans. Veh. Technol.*, vol. 71, no. 5, pp. 4965–4976, 2022.

[28] Z. Zhao, G. Xu, N. Zhang, and Q. Zhang, "Performance analysis of the hybrid satellite-terrestrial relay network with opportunistic scheduling over generalized fading channels," *IEEE Trans. Veh. Technol.*, vol. 71, no. 3, pp. 2914–2924, 2022.

[29] D. Singh and R. Swaminathan, "Comprehensive performance analysis of hybrid FSO/RF space–air–ground integrated network," *Opt. Commun.*, vol. 527, p. 128964, 2023.

[30] K. O. Odeyemi and P. A. Owolawi, "A mixed fso/rf integrated satellite-high altitude platform relaying networks for multiple terrestrial users with presence of eavesdropper: A secrecy performance," in *Photonics*, vol. 9, no. 1, 2022, pp. 1–17.

[31] Y. Ma, T. Lv, G. Pan, Y. Chen, and M.-S. Alouini, "On secure uplink transmission in hybrid RF-FSO cooperative satellite-aerial-terrestrial networks," *IEEE Trans. Commun.*, vol. 70, no. 12, pp. 8244–8257, 2022.

[32] A. Jurado-Navas, J. M. Garrido-Balsells, J. F. Paris, M. Castillo-Vázquez, and A. Puerta-Notario, "Impact of pointing errors on the performance of generalized atmospheric optical channels," *Opt. Express*, vol. 20, no. 11, pp. 12 550–12 562, 2012.

[33] M. R. Aghaei, A. A. Hemmatyar, A. Chamanmotlagh, and M. Fouladian, "Analysis of adaptive multi-rate FSO/RF hybrid systems using Málaga ($\mathcal{M}$) distribution model in turbulent channels," *J. Mod. Opt.*, vol. 67, no. 13, pp. 1159–1169, 2020.

[34] I. S. Gradshteyn and I. M. Ryzhik, *Table of integrals, series, and products*. Academic press, 2014.

[35] A. M. Mathai, R. K. Saxena, and H. J. Haubold, *The H-function: theory and applications*. Springer Science & Business Media, 2009.

[36] G. Zheng, P.-D. Arapoglou, and B. Ottersten, "Physical layer security in multibeam satellite systems," *IEEE Trans. commun.*, vol. 11, no. 2, pp. 852–863, 2011.

[37] K. Guo, K. An, B. Zhang, Y. Huang, and G. Zheng, "Outage analysis of cognitive hybrid satellite-terrestrial networks with hardware impairments and multi-primary users," *IEEE Wireless Commu. Lett.*, vol. 7, no. 5, pp. 816–819, 2018.

[38] K. Balaji and K. Prabu, "Performance evaluation of FSO system using wavelength and time diversity over malaga turbulence channel with pointing errors," *Opt. Commun.*, vol. 410, pp. 643–651, 2018.

[39] N. D. Chatzidiamantis, G. K. Karagiannidis, E. E. Kriezis, and M. Matthaiou, "Diversity combining in hybrid RF/FSO systems with PSK modulation," in *Proc. IEEE Int. Conf. Commun. (ICC)*. IEEE, 2011, pp. 1–6.

[40] B. He and R. Schober, "Bit-interleaved coded modulation for hybrid RF/FSO systems," *IEEE Trans. Commun.*, vol. 57, no. 12, pp. 3753–3763, 2009.

[41] A. A. Kilbas, *H-transforms: Theory and Applications*. CRC press, 2004.

[42] H. A. Suraweera, G. K. Karagiannidis, and P. J. Smith, "Performance analysis of the dual-hop asymmetric fading channel," *IEEE Trans. Wireless Commun.*, vol. 8, no. 6, pp. 2783–2788, 2009.

[43] M. O. Hasna and M.-S. Alouini, "A performance study of dual-hop transmissions with fixed gain relays," *IEEE trans. wireless commun.*, vol. 3, no. 6, pp. 1963–1968, 2004.

[44] M. J. Saber, J. Mazloum, A. M. Sazdar, A. Keshavarz, and M. J. Piran, "On secure mixed RF-FSO decode-and-forward relaying systems with energy harvesting," *IEEE Syst. J.*, vol. 14, no. 3, pp. 4402–4405, 2019.

[45] P. Mittal and K. Gupta, "An integral involving generalized function of two variables," in *Proc. Indian Acad. Sci.-Sec. A*, vol. 75, no. 3. Springer, 1972, pp. 117–123.

[46] Y. Zhang, J. Zhang, L. Yang, B. Ai, and M.-S. Alouini, "On the performance of dual-hop systems over mixed FSO/mmWave fading channels," *IEEE Open J. Commun. Soc.*, vol. 1, pp. 477–489, 2020.

[47] H. Kazemi, M. Uysal, and F. Touati, "Outage analysis of hybrid FSO/RF systems based on finite-state markov chain modeling," in *Int. Workshop in Optical Wireless Commun. (IWOW)*. IEEE, 2014, pp. 11–15.

[48] F. S. Alqurashi, O. Amin, and B. Shihada, "Delay analysis of multi-hop satellite-terrestrial networks with hybrid RF/FSO links," in *Int. Conference on Commun.*, 2023, pp. 2584–2589.